

1 Revised manuscript submitted to *Continental Shelf Research*

2

3 Tracking sea surface salinity and dissolved oxygen on a river-influenced, seasonally stratified
4 shelf, Mississippi Bight, northern Gulf of Mexico

5

6 Brian Dzwonkowski^{1,2}, Severine Fournier³, John T. Reager³, Scott Milroy⁴, Kyeong Park⁵, Alan
7 M. Shiller⁴, Adam T. Greer⁴, Inia Soto^{4,6}, Steven L. Dykstra^{1,2}, and Virginie Sanial⁴

8

9 ¹ Department of Marine Sciences, University of South Alabama, Dauphin Island Sea Lab,
10 Dauphin Island, AL 36528 USA

11 ² Dauphin Island Sea Lab, Dauphin Island, AL 36528 USA

12 ³ Jet Propulsion Laboratory, California Institute of Technology, Pasadena, CA 91109 USA

13 ⁴ Division of Marine Science, University of Southern Mississippi, Stennis Space Center, MS
14 39529 USA

15 ⁵ Department of Marine Sciences, Texas A&M University at Galveston, Galveston, TX 77553
16 USA

17 ⁶ Harte Research Institute, Texas A&M University at Corpus Christi, Corpus Christi, TX 78412
18 USA

19

20 Abstract:

21 River discharge, and its resulting region of freshwater influence (ROFI) in the coastal ocean, has
22 a critical influence on physical and biogeochemical processes in seasonally stratified shelf
23 ecosystems. Multi-year (2010-2016) observations of satellite-derived sea surface salinity (SSS)
24 and *in-situ* water column hydrographic data during summer 2016 were used to investigate
25 physical aspects of the ROFI east of the Mississippi River Delta to better assess regional
26 susceptibility to hypoxia in the summer months. Time series of SSS data indicate that the shelf
27 region impacted by the seasonal expansion of freshwater can be as extensive as the well-known
28 “dead zone” region west of the Delta, and hydrographic observations from a shelf-wide survey
29 indicate strong stratification associated with the ROFI. Peak buoyancy frequencies typically
30 ranged between $0.15\text{-}0.25\text{ s}^{-1}$ and were concentrated in a 2-3 m layer around 4-10 m deep across
31 much of the shelf. This ROFI is expected to be influenced by local freshwater sources which,
32 while individually small, make a notable contribution in aggregate to the region (annually
33 averaged daily discharge of approximately $2880\text{ m}^3\text{ s}^{-1}$). The dissolved oxygen (DO) conditions
34 under this freshwater cap were spatially and temporally variable, with areas of hypoxia and near-
35 hypoxic conditions over portions of the shelf, demonstrating the utility of satellite-derived SSS in
36 identifying coastal areas potential vulnerability to hypoxia. These regions of low bottom
37 dissolved oxygen persisted throughout the peak summer season at several sites on the shelf, with
38 the northeastern corner of Mississippi Bight having the most intense and persistent hypoxia.

39

40 Key words: sea surface salinity, region of freshwater influence, hypoxia, dissolved oxygen,

41 Mississippi Bight, Gulf of Mexico

42

43 1. Introduction

44 Shelf hypoxia (dissolved oxygen $< 2 \text{ mg l}^{-1}$) is a well-recognized management issue for a
45 growing number of coastal regions (Diaz and Rosenberg 2008) that can alter food web dynamics
46 and biogeochemical cycling, resulting in threats to fisheries, coastal economies, and ecosystem
47 health (Breitburg et al. 2009; Diaz and Rosenberg 2011). While hypoxia can occur naturally, the
48 observed or predicted expansion of these conditions in different coastal systems has been linked
49 to several anthropogenic causes, including changes in watershed land use and ocean warming
50 (Rabalais et al. 2009; Bianchi et al. 2010; Dale 2010; Breitburg et al. 2018). One well-studied
51 region with regularly occurring hypoxia is the Louisiana Shelf in the northern Gulf of Mexico,
52 the 2nd largest region of hypoxia globally (Rabalais et al. 2002a). This “dead zone”, typically
53 determined from an annual mid-summer shelf survey, is directly linked to river discharge
54 through the delivery of nutrient-rich water from the Mississippi River watershed and the physical
55 stratification that isolates the bottom water from the oxygenated upper layer (Rabalais et al.
56 1999; Dagg et al. 2007).

57 However, the influence of river discharge in the northern Gulf of Mexico extends well
58 beyond the region typically measured by the annual summer survey. For example, a number of
59 studies have demonstrated eastward spreading of Mississippi River water, which occurs
60 episodically as a result of the passage of weather fronts, or more persistently during periods of
61 southwest winds frequent in the summer season (Walker et al. 1994, 2005; Walker et al. 1996;
62 Hitchcock et al. 1997; Moray et al. 2003a, 2003b; Schiller et al. 2011; Androulidakis and
63 Kourafalou 2013; Kourafalou and Androulidakis 2013; Fournier et al. 2016). These studies
64 typically highlight additional offshore factors, such as the position of the Loop Current and its

65 associated eddies that can also impact the eastward transport of Mississippi River discharge. In
 66 fact, approximately 47% of the Mississippi River water exiting the bird-foot Delta is estimated to
 67 be delivered to the east and/or offshore (U.S. Army Corps of Engineers 1974) as reported by
 68 Dinnel and Wiseman (1986). Additional eastward delivery of Mississippi River water can arise
 69 through anthropogenic intervention, such as the numerous spillways that can be opened to divert
 70 river water during flood events. The Bonnet Carré Spillway is particularly notable as this
 71 opening diverts river water east of the Delta directly into Lake Pontchartrain.

72 In addition to the direct impacts by the Mississippi River water, local sources of riverine
 73 water have the potential to contribute to shelf hypoxia in some coastal regions of the northern
 74 Gulf of Mexico. For example, the Mississippi Bight, a region of freshwater influence (ROFI) to
 75 the east of the Mississippi River Delta, receives river input from numerous local sources in
 76 Louisiana, Mississippi, Alabama, and West Florida (Table 1). While these local sources of river
 77 discharge are individually small, they cumulatively are equivalent to ~44% of the Mississippi
 78 River discharge that is expected to travel eastward or offshore of the Mississippi River Delta,
 79 assuming 30% of the Mississippi River discharge at Vicksburg, MS is diverted into the
 80 Atchafalaya River system (Nittrour et al. 2012) and then ~47% of the remaining discharge travel
 81 offshore or eastward (Army Corps Engineers 1974).

82

83 Table 1. The contribution of local rivers feeding into the Mississippi Sound and Bight relative to the Mississippi
 84 River discharge. The river data is derived from U.S. Geological Survey (USGS) stations between the Mississippi
 85 River Delta in the west and 86.5° W longitude to the east that had a minimum of 1 m³s⁻¹ and 4 complete years of
 86 discharge. The station # is the USGS station number. Discharge represents the annually (Oct-Sep) averaged daily
 87 discharge at each station and the # of years is the number of years associated with the average.

Station name	USGS station #	# of years	Discharge (m ³ s ⁻¹)
--------------	----------------	------------	---------------------------------------------

Mississippi River at Vicksburg, MS	7289000	7	19854
Lake Pontchartrain (^{LP})			109
Amite River near Denham Springs, LA ^{LP, LM}	7378500	78	59
Tickfaw River at Holden, LA ^{LP, LM}	7376000	74	11
Natalbany River at Baptist, LA ^{LP, LM}	7376500	72	3
Tangipahoa River at Robert, LA ^{LP}	7375500	77	32
Tchefuncte River near Folsom, LA ^{LP}	7375000	71	4
Pearl River (^{PR})			338
Pearl River near Bogalusa, LA ^{PR}	2489500	78	282
Bogue Chitto River near Bush, LA ^{PR}	2492000	80	56
Bay St. Louis (^{BL})			24
Catahoula Creek near Santa Rosa, MS ^{BL}	2481570	4	7
Wolf River near Landon, MS ^{BL}	2481510	46	17
Biloxi Bay (^{BB})			10
Biloxi River at Wortham, MS ^{BB}	2481000	63	5
Tuxachanie Creek near Biloxi, MS ^{BB}	2480500	19	5
Pascagoula River (Pas)			357
Pascagoula River at Graham Ferry, MS ^{Pas}	2479310	15	326
Escatawpa near Agricola, MS ^{Pas}	2479560	44	31
Mobile Bay (^{MB})			1726
Tombigbee River at Coffeeville Lock and Dam near Coffeeville, AL ^{MB}	2469761	55	825
Alabama River at Claiborne Lock and Dam near Monroeville, AL ^{MB}	2428400	41	865
Chickasaw Creek near Kushla, AL ^{MB}	2471001	65	8
Fowl River at Half-mile Rd near Laurendine, AL ^{MB}	2471078	19	1
Bassett Creek at Walker Springs, AL ^{MB}	2470100	14	7
Big Flat Creek near Fountain, AL ^{MB}	2428500	27	8
Limestone Creek near Monroeville, AL ^{MB}	2429000	18	4
Little River near Uriah, AL ^{MB}	2429595	11	5
Fish River near Silver Hill, AL ^{MB}	2378500	44	3
Perdido Bay (^{Per})			37
Styx River near Elsanor, AL ^{Per}	2377570	40	12
Perdido River at Barrineau Park, FL ^{Per}	2376500	76	22
Eleven Mile Creek near Pensacola, FL ^{Per}	2376115	30	3
Pensacola Bay (^{Pen})			276
Escambia River near Molino, FL ^{Pen}	2376033	27	184
Pond Creek near Milton, FL ^{Pen}	2370700	25	2
Big Coldwater Creek near Milton, FL ^{Pen}	2370500	68	15
Big Juniper Creek near Munson, FL ^{Pen}	2370200	8	2

Blackwater River near Baker, FL ^{Pen}	2370000	63	10
Yellow River near Milton, FL ^{Pen}	2369600	15	63

88

89 The superscripts associated with each gaging station indicate the primary river/estuary they contribute to: ^{LP} is Lake
90 Pontchartrain, ^{PR} is the Pearl River, ^{BS} is Bay St. Louis, ^{BB} is Bay of Biloxi, ^{Pas} is Pascagoula River, ^{MB} is Mobile
91 Bay, ^{Per} is Perdido Bay, and ^{Pen} is Pensacola Bay. Note ^{LM} indicates the rivers that contribute to Lake Maruepas
92 which in turn feeds into Lake Pontchartrain.

93

94 The impact of high nutrient content and stratifying effects of Mississippi River discharge,
95 as well as other contributing factors (e.g., sediment oxygen demand, grazing rates of
96 microzooplankton) to the west the Mississippi River Delta, have been extensively examined
97 (e.g., Turner and Rabalais 1994; Justić et al., 2003, 2007; Rowe and Chapman 2002; Scavia et
98 al., 2003, 2004; Rabalais et al. 2007; Turner et al. 2007, 2012; Hetland and DiMarco 2008;
99 Lehrter et al. 2009; Liu et al. 2010; Fennel et al. 2011). However, the nutrient loading (one
100 necessary component for development of hypoxia) associated with the local sources of
101 freshwater in the Mississippi Bight is quite different than that of the Mississippi River discharge,
102 which has a much higher nutrient content (Dunn 1996). As a result, the hypoxia-related
103 dynamics in the region to the east of the Delta have been poorly described relative to the adjacent
104 system on the Texas-Louisiana Shelf. In fact, Bianchi et al. (2010) highlighted the frequency of
105 occurrence and spatial extent of hypoxia east of the Mississippi River Delta as an open question
106 in their review of hypoxia dynamics in the northern Gulf of Mexico. The western emphasis of
107 hypoxia has significant policy implications as the most recent hypoxia area reduction plan put
108 forth by the EPA Hypoxia Task Force is based on estimates that do not consider conditions in the
109 Mississippi Bight (US EPA 2008; US EPA 2013; Scavia et al. 2017).

110 To address the need for improved information on the ROFI and associated dissolved
111 oxygen (DO) conditions east of the Mississippi River Delta, this study examines the evolution of
112 surface salinity in the northern Gulf of Mexico and aspects of the DO characteristics in the
113 Mississippi Bight. The development of hypoxic zones results from a combination of respiration
114 depleting DO and physical processes (such as the combination of freshwater and solar heating
115 induced stratification) limiting the equilibration of oxygen with the atmosphere. While both the
116 physical and biogeochemical components of hypoxia are critical, we focus on the physical
117 aspects of this balance in shelf waters of the northern Gulf of Mexico with the broader goal of
118 improving the understanding of drivers contributing to the spatial and temporal patterns of DO in
119 ROFIs, critical ecosystems in the coastal ocean. Specifically, this work highlights the extensive
120 area impacted by freshwater discharge east of the Mississippi River Delta, which is on par with
121 the region to the west of the Delta and demonstrates that satellite-derived SSS is a useful tool in
122 targeting coastal areas that are potentially vulnerable to hypoxia. While the available *in situ* DO
123 data are temporally and spatially limited, there are areas of hypoxia and near-hypoxic conditions
124 in the Mississippi Bight during the stratified season, which highlights the need for this shelf
125 region to be considered in developing future management strategies for the northern Gulf of
126 Mexico.

127

128 2. Methods

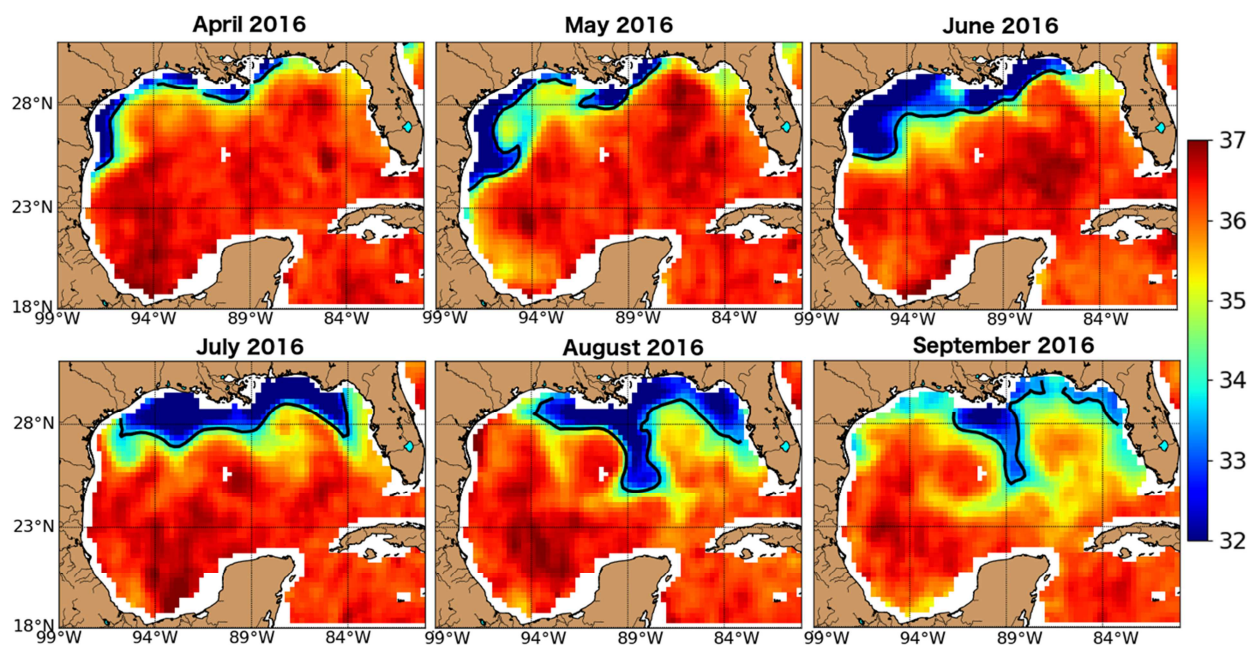
129 2.1 Satellite data

130 For delineating and tracking the evolution of patterns associated with the ROFI in the
131 northern Gulf of Mexico, sea surface salinity (SSS) data were obtained from the European Space
132 Agency (ESA) Soil Moisture Ocean Salinity (SMOS) Earth Explorer mission. The SMOS SSS

133 product used is a level 3, 4-day composite on a $1/4^\circ$ grid (i.e., 25 km spatial resolution) for the
134 2010-2016 period. As a result of this coarse spatial resolution, pixels by the coast are frequently
135 contaminated by land and are excluded from the analysis. These regions are represented by white
136 areas in the SSS plots (Fig. 1). Boutin et al. (2016) showed that the precision of the monthly
137 SMOS SSS measurements are on the order of 0.2 globally when compared with *in situ* data. Note
138 that all salinity values (both satellite-derived and *in situ*) presented are based on the practical
139 salinity scale. Additional details on the SSS product used in this study can be found in Boutin et
140 al. (2018).

141 Time series of monthly averaged SSS maps in the Gulf of Mexico from 2010 to 2016
142 were produced by averaging the gridded L3 4-day composites. From these monthly maps, the
143 ROFI in the northern Gulf of Mexico was delineated by using the 33.5 isohaline contour (Fig. 1).
144 This contour likely indicates some moderate to high level of stratification over the continental
145 shelf and is similar to the salinity contour of 33 and 34 used by Kourafalou and Androulidakis
146 (2013) and Morey et al. (2003a), respectively. Using the 33.5 surface contour as a boundary, the
147 ROFI was then divided into a region east and west of the Mississippi River Delta using the
148 89.5°W longitude line as this is near the eastward edge of the Mississippi River Delta. With the
149 east/west boundary line and the 33.5 contour, coverage areas and mean SSS values within each
150 of the east and west regions were determined. Other contour values and east/west boundary lines
151 were examined but did not qualitatively change the results. Using the 7-yr time series of
152 monthly coverage areas and average salinities for both the east and west regions, a monthly
153 ensemble average was produced. The months of April-September are emphasized to provide
154 some context around the peak stratified period in June-August.

155 The satellite-derived SSS data were complimented with high resolution satellite-derived
 156 ocean color data for July 2016, a time period when several field programs were being conducted
 157 (see Section 2.2). The optical complexity of coastal water can impact the accuracy of standard
 158 ocean color data products in deriving water properties, particularly in river-influenced systems
 159 where colored dissolved organic material and surface inorganic sediments can alter the water
 160 reflectance in the visible bands (e.g., D'Sa et al., 2006; Walker and Rabalais 2006). However,
 161 many studies have qualitatively used 'chlorophyll-a' values from standard ocean color data
 162 products as a proxy for tracking river plumes (e.g., Dzwonkowski and Yan 2005; Walker et al.
 163 2005). For this study, AQUA/MODIS L2 chlorophyll-a data during July 20-26 2016 were
 164 mapped to a 1 km grid and used to provide a qualitative view of riverine/estuarine water relative
 165 to oceanic water during the hydrographic survey period.



166 Figure 1. Spatial structure of the ROFI in the Gulf of Mexico. Sequence of satellite images from
 167 SMOS sensor ($1/4^\circ$ resolution) for sea surface salinity (SSS) showing the evolution of the
 168 horizontal structure of the ROFI in 2016 during the peak stratification period in the northern Gulf
 169 of Mexico. The black line is the 33.5 SSS contour used to delineate the ROFI. The white areas
 170

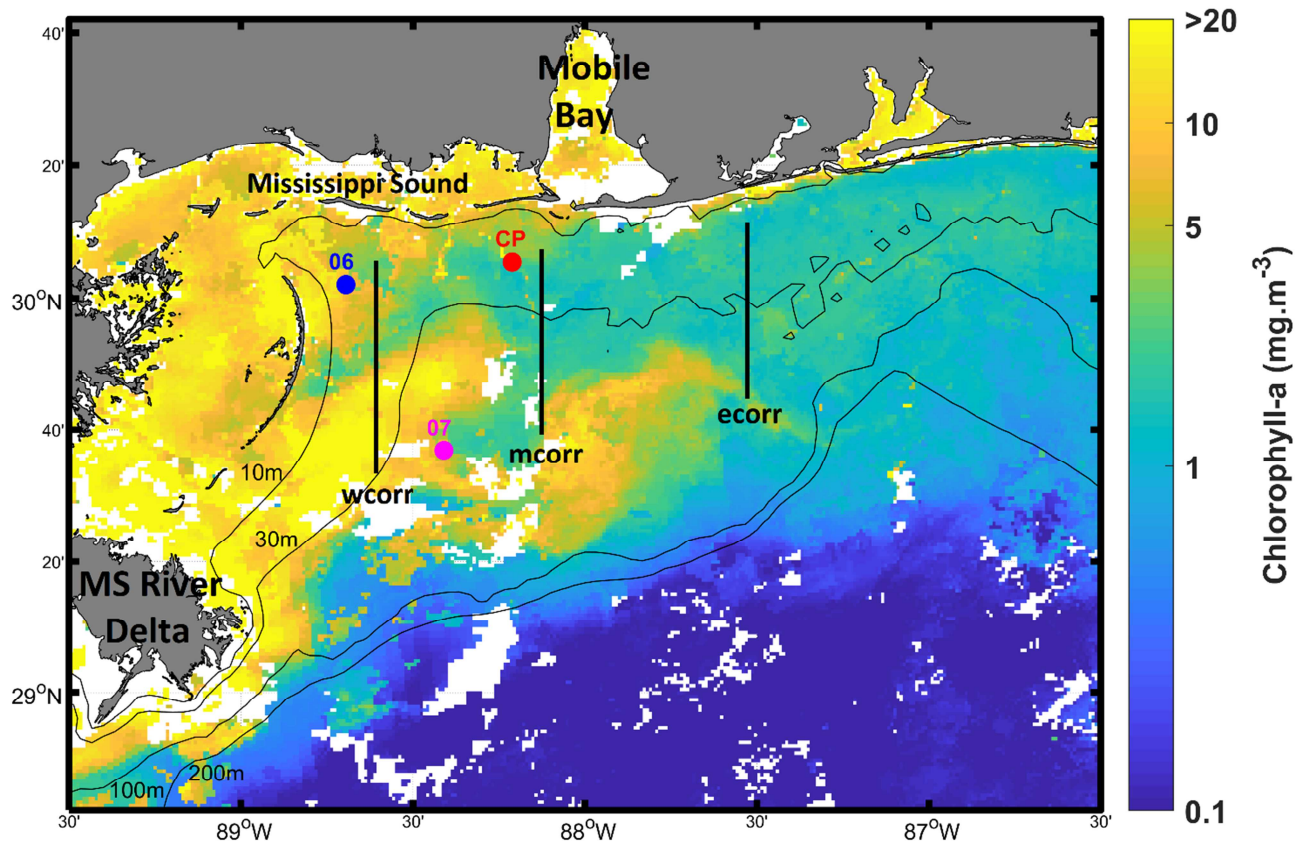
171 adjacent to the coast are pixels that are contaminated by land. Note the lowest value (dark blue)
172 on the color scale is saturated to better highlight the spatial structure in the SSS.

173

174 2.2 Field data

175 To understand the hydrographic conditions associated with the freshwater signal in the
176 SSS data and the patterns of water column DO, field data from the CONSortium for oil spill
177 exposure pathways in COastal River-Dominated Ecosystems (CONCORDE) program (Greer et
178 al. 2018) and several near-bottom mounted DO sensors were obtained for the summer of 2016
179 (Fig. 2). The stratified season of 2016 was emphasized due to the enhanced sampling effort on
180 the shelf during this period. Oceanographic surveys were conducted from the *R/V Point Sur*
181 along three ~50 km north-south lines during July 24–26, 2016. The measurements of
182 temperature, salinity, density and DO were made between ~2 m above the bottom and ~2 m
183 below the surface from a Conductivity-Temperature-Depth (CTD) system attached to the
184 remotely operated towed vehicle known as the *In Situ* Ichthyoplankton Imaging System (ISIIS).
185 The DO sensor on the ISIIS CTD system is a SeaBird Electronics (SBE) 43 and is expected to
186 have an accuracy of $\pm 0.13 \text{ mg l}^{-1}$. Detailed information for sampling and gridding ($\Delta z = 0.2 \text{ m}$
187 and $\Delta x = 200 \text{ m}$) can be found in Dzwonkowski et al. (2017). It is important to note that the
188 deepest ISIIS measurements occur approximately 1.5 meters higher in the water column
189 compared to the DO measurements obtained for the annual hypoxia survey conducted by the
190 Hypoxia Research Team at the Louisiana Universities Marine Consortium (LUMCON:
191 <https://gulfhypoxia.net/>). Additional hourly averaged high frequency near bottom DO data ($\Delta t =$
192 2 to 15 minutes) were obtained from several near bottom HOBO loggers (U26-001; Onset
193 computer, Bourne, MA) deployed at various locations on the shelf (Fig. 2). The logger

194 deployment depths were dependent on available subsurface structures and were generally at or
195 near the bottom with FH06 being ~1.2 m from the bottom in 21.2 m of water, FH07 being ~6.0
196 m from the bottom in 41.1 m of water, and CP being ~0.8 m from the bottom in 20.0 m of water.
197 HOBO loggers were calibrated following manufacturer instructions including pre- and post-
198 deployment assessments. In addition, the DO sensors were deployed with conductivity sensors so
199 that salinity corrections could be made as recommended by the manufacturer, with the exception
200 being site CP, where the CTD sensor failed. However, a validation CTD cast during the
201 sampling period at this site indicated good readings through August 3, 2016, after which data
202 quality degraded. Based on the calibration practices associated with the HOBO loggers the
203 expected error in the DO measurements is $\pm 0.2 \text{ mg l}^{-1}$. Daily discharge data were obtained for the
204 Mississippi River at the USGS station at Vicksburg, MS and for the Mobile River system at two
205 USGS stations for the Alabama River and Tombigbee River, which represent the vast majority of
206 river water flowing into Mobile Bay (Table 1).



207
 208 Figure 2. Mississippi Bight region with the CONCORDE 2016 summer survey transects
 209 (labelled thick black lines) and selected times series locations of bottom dissolved oxygen
 210 (circles). Bathymetry contours highlight shelf structure (black lines). Coloration is 7-d average of
 211 chlorophyll-a derived from MODIS sensor (1 km resolution) for the week of July 20-26, 2016.
 212 Due to the optical complexity of coastal waters, the chlorophyll-a concentration represents
 213 relative values but effectively illustrates an intrusion of fresher water (yellow filament) on the
 214 shelf.

215

216 3. Results

217 3.1 Horizontal extent of the ROFI

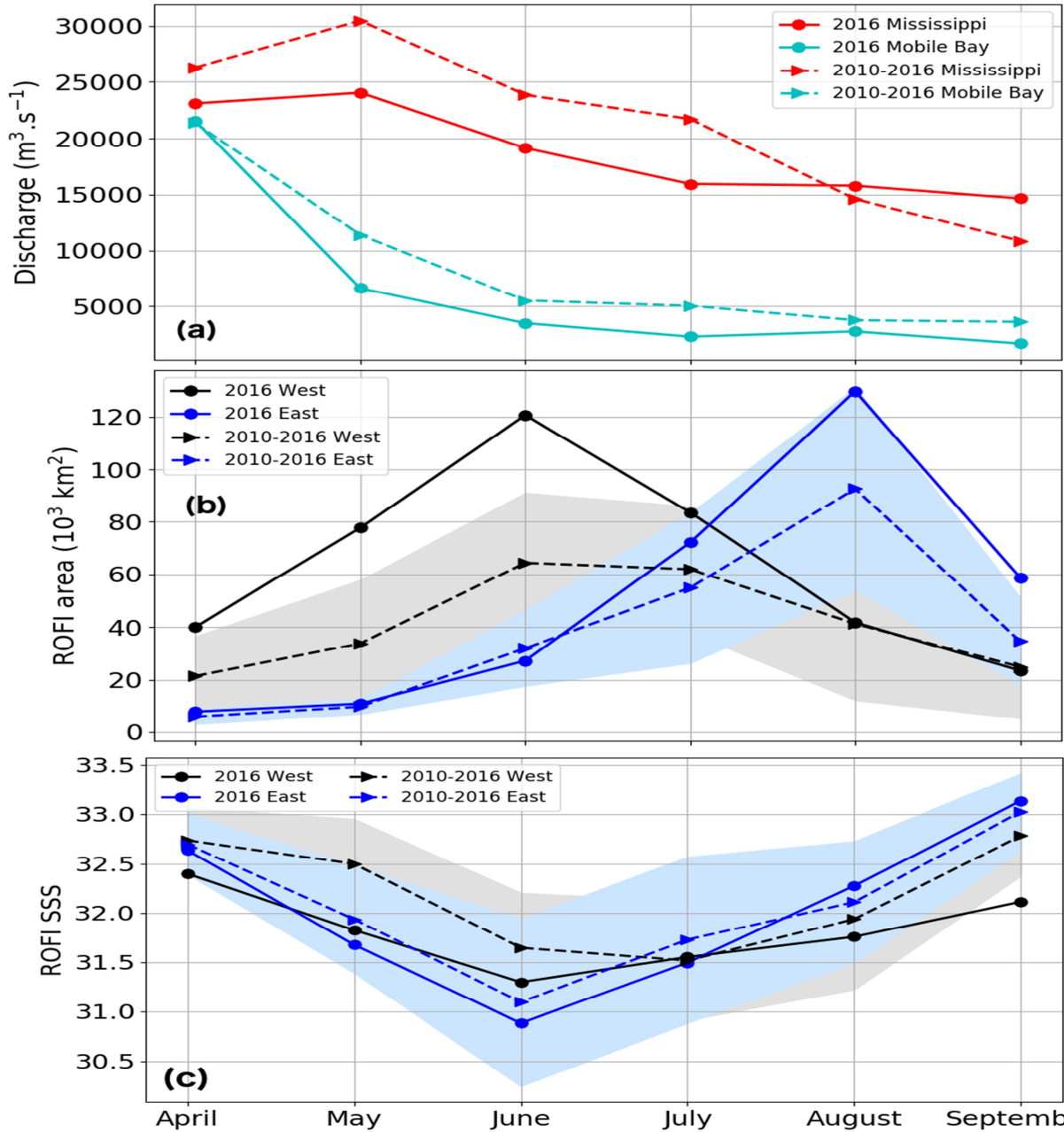
218 SSS data for the stratified seasons from late spring to early fall showed the freshwater
 219 signal throughout the Gulf of Mexico (Fig. 1). As evidenced in the imagery, freshwater inputs to

220 the northern Gulf of Mexico were present throughout the study period, and there was a
221 significant freshening on the shelf relative to offshore across the entire northern Gulf of Mexico.
222 The temporal and spatial evolution of the ROFI were quantified using the coverage area and
223 mean SSS to characterize the relative impact of this feature to the east and west of the
224 Mississippi River Delta (Fig. 3). The ROFIs to the east and west of the Mississippi River Delta
225 expanded rapidly from April to mid/late summer in 2016, increasing from 40×10^3 to 120×10^3
226 km^2 for the western region and 7×10^3 to $130 \times 10^3 \text{ km}^2$ for the eastern region. While the overall
227 size of these regions was similar, the timing of the peak period was offset by two months, with
228 the western (eastern) region peaking in June (August). Interestingly, the rates of expansion (i.e.,
229 the slope of the line from April to June for the western region and from June to August for the
230 eastern region) were similar. Note that the phase lag in growth was not mirrored by enhanced
231 river discharge from local sources. Mobile Bay, the largest local system delivering freshwater
232 into the Mississippi Bight, peaked well before the August peak of the eastern ROFI, which
233 suggests that advective processes may be important for the summer expansion of freshwater.

234 Mean SSS decreased in connection with increasing spatial coverage of freshwater
235 discharge. Both regions had similar surface salinity beginning with values of ~ 32.5 in April and
236 decreased to a summer minimum in June of ~ 31 . The month of September had a particularly
237 sharp decline in coverage area in the eastern region ($\sim 54\%$ reduction) and a notable increase in
238 mean salinity (32.3 to 33.1). Overall, the ROFIs to the west and east of the Mississippi River
239 Delta were similar in size and mean salinity during peak summer months (June-August) of 2016.

240 Considering the potential for large interannual variability, the stratified season in 2016
241 was compared to the 7-yr (2010-2016) ensemble averaged characteristics of the ROFI to evaluate
242 whether the observed conditions in 2016 were representative of typical patterns on the shelf and

243 adjacent waters. In terms of the coverage area and mean salinity, their time evolution in 2016
244 was similar to the ensemble averaged conditions in both regions. In both the western and eastern
245 regions, the overall size and freshening were larger in 2016 when compared to the ensemble
246 averages. In addition to placing the 2016 conditions within the context of long term patterns, the
247 ensemble averaged characteristics highlighted the broader patterns of the two zones of the ROFI.
248 Focusing on the peak summer months (June-August), the mean characteristics were similar with
249 mean coverage areas of $60(\pm 14) \times 10^3 \text{ km}^2$ (east) and $56(\pm 11) \times 10^3 \text{ km}^2$ (west), as well as mean
250 salinities of $31.6(\pm 0.3)$ (east) and $31.6(\pm 0.2)$ (west). These results indicated that the size of the
251 ROFI in the eastern region typically had a coverage area and mean SSS similar to those of the
252 western region during the peak stratification period in June-August.



253

254

255

256

257

258

259

260

261

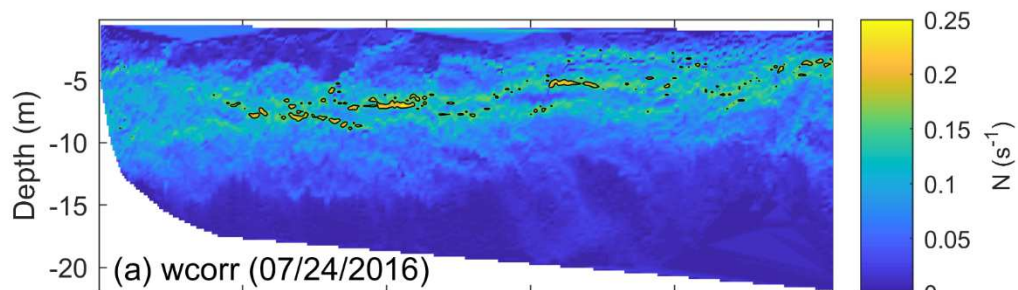
Figure 3. Time series of the (a) river discharge for Mississippi River and Mobile Bay (*scaled up by a factor of 8*), and the (b) coverage area and (c) mean SSS in the ROFI to the east and west of the Mississippi River Delta: the monthly values in 2016 (solid lines) and the 7-yr ensemble averages (dashed lines) ± 1 standard deviation (shaded). The ROFI is defined by the region with the 33.5 SSS contour and the east and west regions are determined by the 89.5°W longitude, i.e., approximate location of the Mississippi River Delta.

262

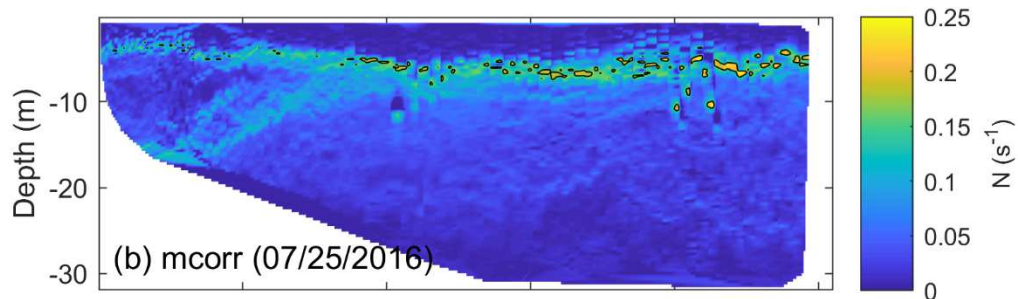
263 3.2 Shelf stratification

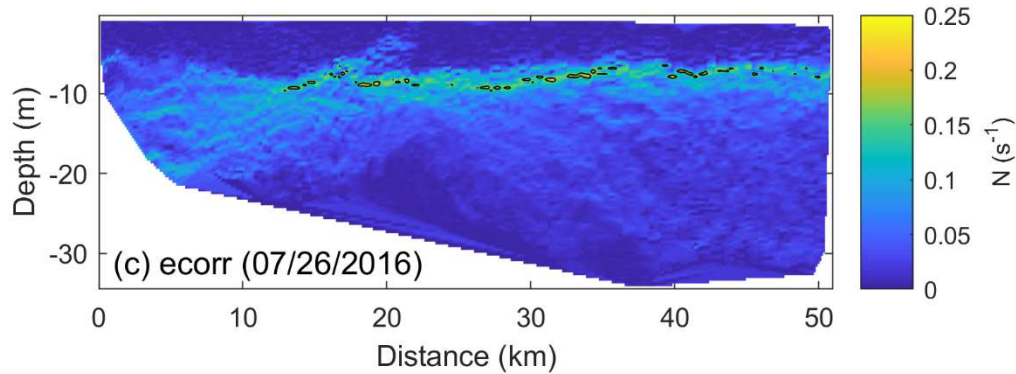
264 The vertical structure of the large ROFI to the east of the Mississippi River Delta was
265 examined with data from the CONCORDE survey lines. In general, this region of the ROFI had
266 a strong freshwater lens, with surface to bottom salinity differences typically on the order of 5-8
267 across the shelf. These salinity gradients, coupled with temperature gradients (see supplemental
268 material), resulted in strong vertical density gradients (Fig. 4) with corresponding high buoyancy
269 frequencies (N) (Fig. 4). Peak buoyancy frequencies typically ranged between $0.15\text{-}0.25\text{ s}^{-1}$ and
270 were concentrated in a 2-3 m layer of the water column around 4-10 m deep across much of the
271 shelf, except near the coast where the pycnocline broke down. The change in stratification near
272 the coast resulted from a strong wind-driven downwelling event (not shown) which modified the
273 density structure tilting the isopycnals downward and offshore (i.e., Fig. 5b,c).

274



275



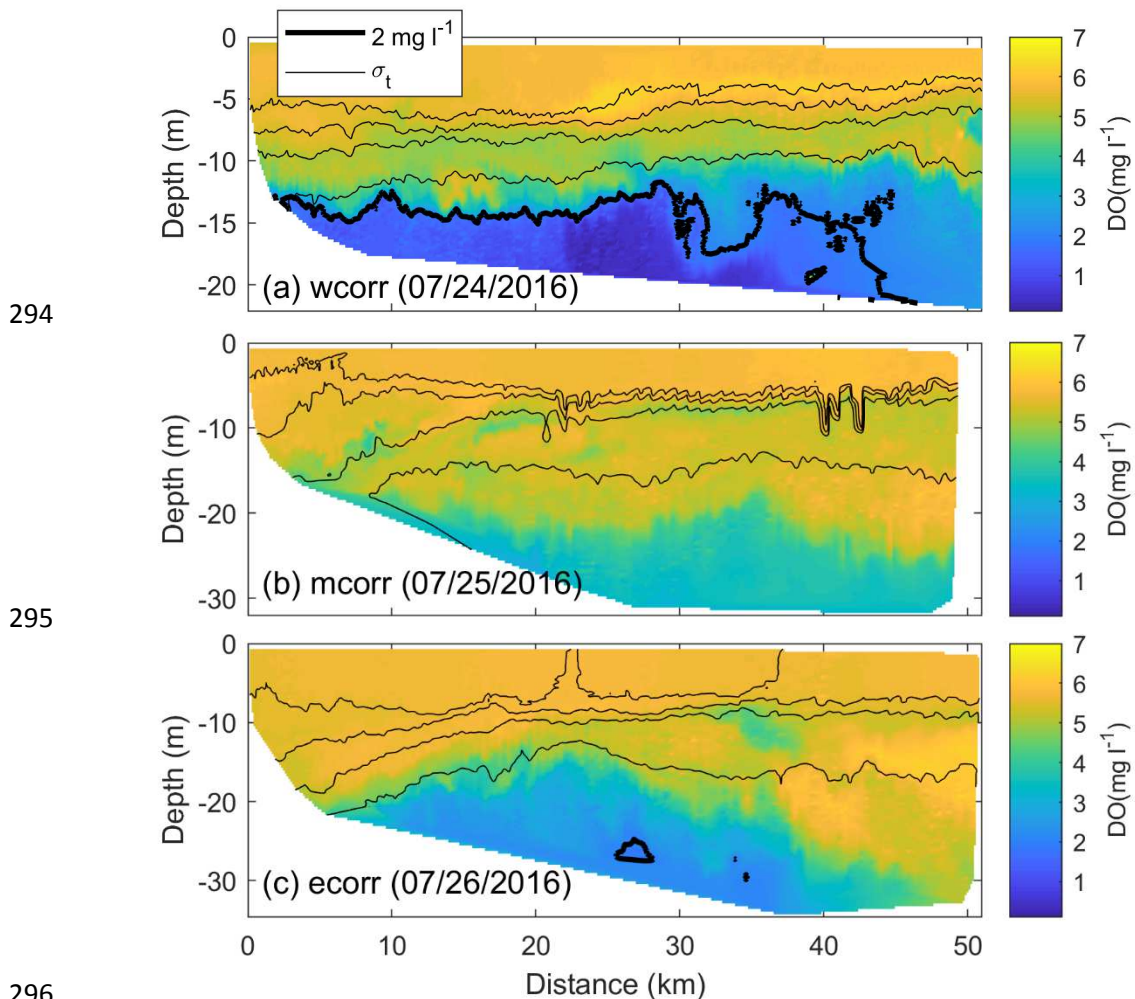


276
 277 Figure 4. Across-shelf transects of buoyancy frequency from the ISIS towed CTD sensor for (a)
 278 wcorr, (b) mcorr, and (c) ecorr on July 24, July 25, and July 26 2016, respectively (see Fig. 2 for
 279 locations of transects). The black contour highlights buoyancy frequencies above 0.17 s^{-1} . Note
 280 the change in the y-axis in (b) and (c)

281

282 3.3 Dissolved oxygen on the shelf

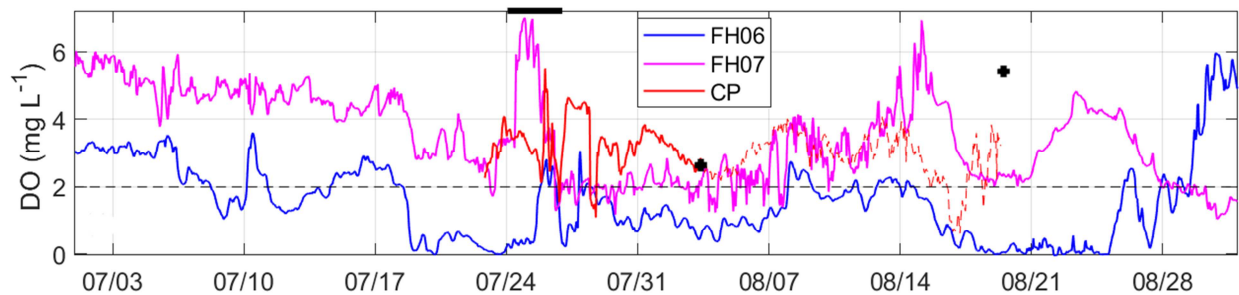
283 While all three transects had generally high levels of stratification, the water column DO
 284 patterns varied spatially (Fig. 5). Clearly, wcorr had the lowest DO levels, with hypoxic
 285 conditions covering the majority of the bottom layer deeper than $\sim 13 \text{ m}$. In contrast, the mcorr
 286 and ecorr transects were generally not hypoxic, although both transects still had low levels of DO
 287 with near-bottom values ranging from $2\text{-}3 \text{ mg l}^{-1}$. Interestingly, ecorr had somewhat lower
 288 values than mcorr with various patches of near-bottom DO being at or just below 2 mg l^{-1} . The
 289 nearshore end of all the transects had elevated DO, relative to offshore locations, due to mixing
 290 and downward advection of surface waters from a downwelling event during the survey period.
 291 It is worth noting that the ISIS instrument undulates throughout the water column staying of ~ 2
 292 m above the bottom so the DO level at the bottom may be lower than the values captured along
 293 the transect.



296
 297
 298 Figure 5. Across-shelf transects of DO (coloration) and density (thin contours for the 18, 20, 22
 299 and 24 σ_t levels) from the ISIIS towed CTD sensor for (a) wcorr, (b) mcorr, and (c) ecorr on July
 300 24, July 25, and July 26 2016, respectively (See Fig. 2 for locations of transects). In (a) and (c),
 301 the thick black lines are DO contours for 2 mg l^{-1} . Note the change in the y-axis in (b) and (c).

302
 303 Time series data of DO (Fig. 6) were consistent with the spatial structure in the survey
 304 data. The site FH06 in the northwest corner of the Mississippi Bight generally had the most
 305 frequent and intense hypoxic periods. Waters in the eastern-most and southern-most sites (CP
 306 and FH07, respectively) were generally not hypoxic, hovering between $2\text{-}4 \text{ mg l}^{-1}$ for long time

307 periods (~5-15 day episodes). These observations were spatially consistent with the ship survey
 308 data. The fact the waters at the FH07 station were at or near hypoxic despite being ~6.0 m off
 309 the bottom indicate there is a likely a thick layer of layer of low DO (and potential hypoxic
 310 values at the bottom) in this region of Mississippi Bight. The time series data also highlight the
 311 fact that the ship survey occurred during a period of elevated DO values, likely associated with
 312 the strong downwelling event. Rather than a straightforward trend of decreasing DO with
 313 distance from the Mississippi River Delta, the transects and time series data reveal more complex
 314 patterns.



315
 316
 317 Fig. 6. Time series of DO at three sites: FH06, FH07 and CP (see Fig. 2 for locations). The
 318 horizontal black line at the top indicates the survey period and the black crosses are independent
 319 measurements of DO at site CP with the red dashed line showing the DO data with degraded data
 320 quality. Note the FH07 is 6m above the bottom but still within the lower 15% of the water
 321 column.

323 4. Discussion

324 4.1 Physical characterization of Mississippi Bight

325 While the fine-scale details of the regional river plumes cannot be captured by the coarse
 326 resolution of the SMOS data, the imagery provides the broader structure and an indication of the
 327 intensity of the ROFI in the northern Gulf of Mexico. As might be expected from previous work

328 in the northern Gulf of Mexico (e.g., Rabalais et al. 2002b), the SSS data in 2016 showed a broad
329 region of low salinity water to the west of the Mississippi River Delta that expanded and
330 intensified through the summer months. However, the SSS imagery clearly showed the region to
331 the east of the Mississippi River Delta also had an expansive ROFI over the shelf. Physical
332 processes associated with this freshwater expansion have been examined in previous studies
333 (e.g., Walker et al. 1994; Weisberg 1994; Morey et al. 2003a, 2003b; Schiller et al. 2011;
334 Fournier et al. 2016); however, the multi-year record of satellite SSS provides a novel, spatially
335 synoptic view of salinity characteristics of this region. The timing of the eastward expansion of
336 fresher water and the associated time lag (2 months relative to the western ROFI in Fig. 3b) are
337 consistent with the previous work mentioned above that linked the seasonal southwest winds
338 with the eastward advection of Mississippi River water. In addition, freshwater from local
339 sources in Louisiana, Mississippi, Alabama, and the Florida Panhandle would also be expected to
340 be advected eastward as the seasonal inner/mid-shelf circulation is similarly eastward in the
341 summer (Dzwonkowski and Park 2010). Rather surprisingly, the ROFI coverage area and mean
342 SSS to the east of the Mississippi River Delta are similar to those to the west of the Delta.

343 Combining satellite and *in situ* data during summer 2016 provides insight into the effects
344 of this freshwater signal on shelf stratification and DO patterns. The available salinity and
345 density data from within this ROFI showed a stratified water column with high buoyancy
346 frequencies in the pycnocline, $O(0.15 \text{ s}^{-1})$, across the shelf. While Belabbassi (2006) reported
347 bottom hypoxia in the ‘Dead Zone’ region on the Texas-Louisiana shelf was associated with
348 buoyancy frequency values greater 0.17 s^{-1} , this was not always the case in the Mississippi Bight
349 (Fig. 4 and Fig. 5). The transect data also highlighted important features in the spatial structure
350 of the stratification on the shelf where a downwelling event, a typical summer phenomenon in

351 this region (Dzwonkowski and Park 2012), modified the nearshore density structure, likely
352 oxygenating much of the nearshore region of the coast.

353 Given the relatively average levels of river discharge from the Mississippi River and
354 Mobile Bay (Fig. 3a) as well as the lack of tropical storm activity during the summer 2016, the
355 ship transects are likely representative of shelf hydrographic conditions in the Mississippi Bight.
356 The observed stratification levels in 2016 are consistent with previous regional work of water
357 column stability that have measured buoyancy frequencies on the order of $0.07\text{-}0.20\text{ s}^{-1}$
358 (Belabbassi 2006; Dzwonkowski et al. 2018), similar to conditions observed on the Texas-
359 Louisiana Shelf, i.e., buoyancy frequencies $\sim 0.07\text{-}0.28\text{ s}^{-1}$ (Wiseman et al. 1997; Belabbassi
360 2006; Bianchi et al. 2010). However, the sources of the shelf stratification in the Mississippi
361 Bight appear less straightforward. The Mississippi River discharge is much larger than the
362 Mobile Bay discharge (Fig. 3a) and should be an important source of buoyancy on the shelf. In
363 contrast, recent stable isotope work has indicated that local river sources, including the Mobile
364 Bay discharge and smaller rivers in Mississippi, are the primary contributors of freshwater to the
365 Mississippi Bight (Greer et al. 2018; Sanial et al. submitted). This suggest that the smaller local
366 sources of river discharge might be more important to the physical structuring of inner to mid-
367 shelf region than previously recognized, consistent with the findings of Greer et al. (2018).

368

369 4.2 Biogeochemical implications for the Mississippi Bight

370 Both the Mississippi Bight and Texas-Louisiana shelf have broad ROFIs with high levels
371 of freshwater-derived stratification and limited physical mechanisms capable of enhancing
372 vertical exchange between the surface and bottom waters during the summer months. This
373 suggests the potential for large areas of shelf hypoxia to the east of the Mississippi River Delta.

374 There are a few previous studies that focused on the hypoxia on the shallower regions of the
375 Mississippi/Alabama shelf (e.g., Turner et al. 1987; Brunner et al. 2006; Milroy 2016;
376 Gunderson et al. in revision), but not much is known about the spatial extent or temporal
377 duration/frequency of the hypoxic conditions over the entire Mississippi Bight. Moshogianis et
378 al. (2013) provided a map for the spatial extent of hypoxia of about 2,720 km² in the Mississippi
379 Bight in July 2011 but acknowledged that the actual hypoxic zone was most likely larger as the
380 data collection did not extend past the Mississippi/Alabama border. Hypoxia was also observed
381 in Mississippi Bight during the 2011 annual hypoxia mapping conducted by LUMCON
382 (https://gulfhypoxia.net/research/shelfwide-cruise/?y=2011&p=oxygen_maps) whose sampling
383 survey was atypically extended into this region. Greer et al. (2016) also reported hypoxia in the
384 Mississippi Bight in 2011 to the east of River Delta (i.e., south of the wcorr transect).
385 Rakocinski and Menke (2016) mapped the hypoxic zone in the summer of 2008 that was
386 similarly limited by the spatial coverage of the survey. Jochens et al. (2002) provided some
387 limited coverage across the Mississippi Bight but found no hypoxia on the shelf and only limited
388 low DO on summer surveys during 1998-2000. In contrast, results presented here found areas of
389 hypoxic/near-hypoxic conditions (2.0-2.5 mg l⁻¹) on the shelf as far east as 87.53° W, i.e., east of
390 Mobile Bay mouth.

391 While the similar physical conditions are expected to provide the same potential for
392 hypoxia, there might be considerable differences in the biogeochemical conditions between the
393 ROFIs to the west and east of the Mississippi River Delta. The contribution of local rivers to the
394 freshwater on the shelf is likely to be an important consideration, as the nutrient concentrations
395 associated with these systems are much smaller than those in the Mississippi River (Dunn 1996).
396 Thus, if the Mississippi Bight indeed receives a lower supply of fluvial nutrients relative to the

397 Louisiana Shelf, then either the Bight has a lower biogeochemical potential for hypoxia than the
398 Louisiana Shelf, or the Bight has an additional source of allochthonous nutrients. For
399 example, Montiel et al. (pers. comm.) highlight the importance of nutrient fluxes delivered to
400 Mobile Bay by submarine groundwater discharge (SGD), which accounts for 51% of the total
401 ammonium budget and 22% of the total nitrogen input during the low river flow regime,
402 characteristic of the summer season. In other areas where hypoxia is directly connected to
403 sewage treatment runoff, nutrient reductions have led to a coincident reduction in hypoxia,
404 increased water clarity, and recovery of seagrass beds (Kemp et al. 2009; Greening et al. 2014;
405 Staehr et al. 2017). However, some time series studies have shown nutrient reductions leading to
406 biological community changes but no corresponding reduction in hypoxia, which can be
407 attributed primarily to increasing stratification throughout the time series or changing rates of
408 filtration (Kemp et al. 2009; Riemann et al. 2016). Clearly, the physical conditions have an
409 impact on hypoxia intensity and coverage (Oviatt et al. 2017), especially in larger, more diffuse
410 ROFIs (Kemp et al. 2009), but the details involving the interactions between the physical
411 conditions, biological responses, and resulting hypoxia will remain important research topics in
412 order to improve interannual predictability of hypoxia in ROFIs.

413 Another consideration is the episodic eastward advection of Mississippi River discharge,
414 a typical summer phenomenon (e.g., Morey et al. 2003b), that contributes to the late summer
415 expansion of the eastern ROFI. The role of this input on shelf hypoxia patterns in the
416 Mississippi Bight has not been clearly determined. During the CONCORDE surveys, the wcorr
417 transect had the largest area of hypoxia observed, but the near-bottom DO actually decreased in
418 the direction of the Mississippi River Delta. In fact, the transect and time series data during 2016
419 suggest that the intensity and persistence of hypoxia decreased with distance away from the

420 northwest corner of the Mississippi Bight, which is consistent with limited monitoring efforts
421 across several programs and over a number of years (John Lopez and Stephan Howden, pers.
422 comm.). However, there is likely significant interannual variability in the impact of Mississippi
423 River water on the Mississippi Bight hypoxia patterns, as other previous work shows hypoxia
424 closer to the Mississippi River Delta (e.g., Greer et al. 2016).

425 An additional consideration is the opening of the Bonnet Carré Spillway. While this is
426 does not occur frequently, timing of the openings maybe important on the system hypoxia
427 dynamics. During 2016, the Bonnet Carré Spillway was opened in January as a result of a large
428 and relatively uncommon winter flooding event. Work by the CONCORDE program indicated
429 much of the freshwater associated with this event was advected southward out of the Mississippi
430 Bight region, consistent with the typically seasonal southwestward circulation patterns (Mustafa
431 Kemal Cambazoglu, pers. comm.). However, potential biogeochemical impacts on summer
432 hypoxia remains uncertain.

433

434 5. Conclusions

435 This study investigated relationships between river discharge, stratification, and DO
436 patterns on a seasonally stratified shelf system, with a focus on water column properties in the
437 ROFI east of the Mississippi River Delta. The satellite-derived SSS data provided evidence that
438 the ROFI east of the Mississippi River Delta is similar in size and average salinity to the one
439 west of the Mississippi River Delta. Local sources, while individually small, make a significant
440 freshwater contribution in aggregate to the Mississippi Bight region (annually averaged daily
441 discharge of approximately $2880 \text{ m}^3 \text{ s}^{-1}$). While Mobile Bay is the largest contributor

442 (approximately 60%) to the collective total, several other riverine/estuarine systems are also
443 notable including the Pascagoula River, Pearl River, Pensacola Bay, and Lake Pontchartrain.

444 With observations from *in situ* sampling programs in 2016, stratification and DO for a
445 portion of the east ROFI were analyzed to characterize the temporal and spatial structure of the
446 DO patterns. Despite strong stratification over much of the shelf, the ship surveys and time
447 series data demonstrated variability in the horizontal and vertical structure of the DO patterns,
448 with persistent hypoxia occurring in the northwest corner region of the Mississippi Bight and
449 near-hypoxic waters widespread across the shelf during summer. Importantly, even though the
450 eastern portion of the study region appears to be less hypoxic relative to the western portion of
451 the Mississippi Bight and Texas-Louisiana shelf, the low DO levels observed, as well as the
452 extensive ROFI that serves as a “cap” preventing deep waters from equilibrating with the
453 atmosphere, suggest this region may be highly susceptible to becoming hypoxic should there be
454 changes to background environmental conditions (e.g., increased ocean warming), regional
455 watershed land use (e.g., coastal urbanization), or outflow pathways of freshwater discharge
456 (e.g., increased discharge through spillways or erosional loss of the Mississippi River Delta).
457 While the physical conditions in the east ROFI appear to be similar to those of the west ROFI, it
458 is unclear whether the same biogeochemical processes may be at work. This raises broader
459 questions about the factors impacting the oxygen budgets on the shelf and the relationships
460 between freshwater-derived stratification, differing nutrient loads/sources, and biological
461 interactions in river-influenced systems.

462

463 Acknowledgements - This work would not have been possible without the help of the Tech
464 Support Group at the Dauphin Island Sea Lab and CONCORDE summer survey team. We thank

465 Rich Pawlowicz at the University of British Columbia for the freely available MATLAB m_map
466 toolbox. This research was made possible in part by a grant from The Gulf of Mexico Research
467 Initiative, and in part by grants from the NASA SUSMAP program and the National Fish and
468 Wildlife Foundation (NFWF). Data are publicly available through the Gulf of Mexico Research
469 Initiative Information & Data Cooperative (GRIIDC) at <https://data.gulfresearchinitiative.org>
470 (doi:10.7266/N75T3HXP, doi:10.7266/N7QV3JXD). A portion of this work was conducted at
471 the Jet Propulsion Laboratory, California Institute of Technology, under contract with NASA.
472 We thank the NASA Goddard Space Flight Center, Ocean Ecology Laboratory, Ocean Biology
473 Processing Group for the Moderate- resolution Imaging Spectroradiometer (MODIS) Aqua
474 ocean color data; 2014 Reprocessing. NASA OB.DAAC, Greenbelt, MD, USA.
475 doi:10.5067/AQUA/MODIS/MODIS_OC.2014.0. Other data used for this manuscript are
476 publicly available from various sources, including <http://www.mymobilebay.com/> and the
477 CNES-IFREMER CATDS for SMOS SSS data (<http://www.catds.fr/>).

478

479 References

- 480 Androulidakis, Y.S. and V.H. Kourafalou. 2013. On the processes that influence the transport
481 and fate of Mississippi waters under flooding outflow conditions. *Ocean Dyn.*, 63(2-3),
482 143-164.
- 483 Belabbassi, L. 2006. Examination of the relationship of river water to occurrences of bottom
484 water with reduced oxygen concentrations in the northern Gulf of Mexico. Ph.D.
485 Dissertation, Texas A&M University, College Station, TX.

486 Bianchi, T.S., S.F. DiMarco, J.H. Cowan Jr, R.D. Hetland, P. Chapman, J.W. Day and M.A.
487 Allison. 2010. The science of hypoxia in the Northern Gulf of Mexico: a review. *Sci. of*
488 *Total Environ.*, 408(7), 1471-1484.

489 Boutin J., N. Martin, N. Kolodziejczyk and G. Reverdin. 2016. Interannual anomalies of SMOS
490 sea surface salinity, *Rem. Sensing Env.*, 180, 128-136.

491 Boutin, J., J.-L. Vergely, S. Marchand, F. D'Amico, A. Hasson, N. Kolodziejczyk, N. Reul, G.
492 Reverdin and J. Vialard. 2018. New SMOS sea surface salinity with reduced systematic
493 errors and improved variability. *Rem. Sensing Env.*, 214, 115-134.

494 Breitburg, D., D.W. Hondorp, L.A. Davias, and R.J. Diaz. 2009. Hypoxia, nitrogen, and
495 fisheries: integrating effects across local and global landscapes. *Annu. Rev. Mar. Sci.*,
496 1,329-349.

497 Breitburg, D., and others, 2018. Declining oxygen in the global ocean and coastal waters.
498 *Science*, 359(6371), 7240.

499 Brunner, C.A., J.M. Beall, S.J. Bentley and Y. Furukawa. 2006. Hypoxia hotspots in the
500 Mississippi Bight. *J. Foraminiferal Res.*, 36(2), 95-107.

501 Dagg M.J., J.W. Ammerman, R.M.W. Amon, W.S. Gardner, R.E. Green, and S.E. Lohrenz.
502 2007. A review of water column processes influencing hypoxia in the northern Gulf of
503 Mexico. *Estuaries Coasts*, 30(5), 735-52.

504 Dale, V.H. and others. 2010. *Hypoxia in the Northern Gulf of Mexico*. New York: Springer.

505 Diaz, R.J. and R. Rosenberg. 2008. Spreading dead zones and consequences for marine
506 ecosystems. *Science*, 321(5891), 926-929.

507 Diaz, R.J. and R. Rosenberg. 2011. Introduction to environmental and economic consequences of
508 hypoxia. *International Journal of Water Resources Development*, 27(1), 71-82.

509 Dinnel, S.P. and W.J. Wiseman Jr. 1986. Fresh water on the Louisiana and Texas shelf. *Cont.*
510 *Shelf Res.*, 6(6), 765-784.

511 Dunn, D.E., 1996. Trends in Nutrient Inflows to the Gulf of Mexico from Streams Draining the
512 Conterminous United States, 1972-93. Water-Resources Investigations Report 96-4113,
513 U.S. Geological Survey.

514 D'Sa, E. J., R. L. Miller and C. Del Castillo. 2006. Bio-optical properties and ocean color
515 algorithms for coastal waters influenced by the Mississippi River during a cold front,
516 *Applied Optics*, 45(28), 7410-7428.

517 Dzwonkowski, B. and X.H. Yan. 2005. Tracking of a Chesapeake Bay estuarine outflow plume
518 with satellite-based ocean color data. *Cont. Shelf Res.* 25(16), 1942-1958.

519 Dzwonkowski, B. and K. Park. 2010. Influence of wind stress and discharge on the mean and
520 seasonal currents on the Alabama shelf of the northeastern Gulf of Mexico. *J. Geophys.*
521 *Res.: Oceans*, 115, C12052, doi:10.1029/2010JC006449.

522 Dzwonkowski, B. and K. Park. 2012. Subtidal circulation on the Alabama shelf during the
523 Deepwater Horizon oil spill. *J. Geophys. Res.: Oceans*, 117, C03027,
524 doi:10.1029/2011JC007664.

525 Dzwonkowski, B. and others. 2017. Estuarine influence on biogeochemical properties of the
526 Alabama shelf during the fall season. *Cont. Shelf Res.*, 140(15), 96-109, doi:
527 10.1016/j.csr.2017.05.001.

528 Dzwonkowski, B., S. Fournier, K. Park, S. Dykstra and J.T. Reager. 2018. Water column
529 stability and the role of velocity shear on a seasonally stratified shelf, Mississippi Bight,
530 Northern Gulf of Mexico. *J. Geophys. Res.: Oceans*, 123, doi:10.1029/2017JC013624.

531 US EPA, 2008. Gulf of Mexico Action Plan, 2008. <https://www.epa.gov/ms-htf/gulf-hypoxia->
532 [action-plan-2008](https://www.epa.gov/ms-htf/gulf-hypoxia-action-plan-2008).

533 US EPA, 2013. Reassessment 2013: Assessing Progress Made Since 2008.
534 <https://www.epa.gov/ms-htf/hypoxia-task-force-reassessment-2013-assessing-progress->
535 [made-2008](https://www.epa.gov/ms-htf/hypoxia-task-force-reassessment-2013-assessing-progress-made-2008).

536 Fennel, K., R. Hetland, Y. Feng and S. DiMarco. 2011. A coupled physical–biological model of
537 the northern Gulf of Mexico shelf: Model description, validation and analysis of
538 phytoplankton variability. *Biogeosciences* 8,1811–1899.

539 Fournier, S., J.T. Reager, T. Lee, J. Vazquez-Cuervo, C.H. David and M.M. Gierach. 2016.
540 SMAP observes flooding from land to sea: The Texas event of 2015. *Geophys. Res. Lett.*,
541 43(19), 10338-10346.

542 Greening, H., A. Janicki, E. T. Sherwood, R. Pribble, and J. O. R. Johansson. 2014. Ecosystem
543 responses to long-term nutrient management in an urban estuary: Tampa Bay, Florida,
544 USA. *Estuarine, Coastal and Shelf Science*, 151, A1-A16.

545 Greer, A.T., C.B. Woodson, C.E. Smith, C.M. Guigand and R.K. Cowen. 2016. Examining
546 mesozooplankton patch structure and its implications for trophic interactions in the
547 northern Gulf of Mexico. *J. Plankton Res.*, 38(4), 1115-1134.

548 Greer, A.T. and others. 2018. Functioning of coastal river-dominated ecosystems and
549 implications for oil spill response: From observations to mechanisms and models.
550 *Oceanogr.*, 31(3), <https://doi.org/10.5670/oceanog.2018.302>.

551 Gunderson, K., K. Dillion, S. Howden and K. Martin. In Revision. River discharge, stratification
552 and shelf water hypoxia in the Mississippi Bight, *Estuaries Coasts*.

553 Hetland, R.D. and S.F. DiMarco. 2008. How does the character of oxygen demand control the
554 structure of hypoxia on the Texas–Louisiana continental shelf. *J. of Mar. Syst.* 70(1–2),
555 49–62.

556 Hitchcock, G.L., W.J. Wiseman Jr., W.C. Boicourt, A.J. Mariano, N. Walker, T.A. Nelsen and E.
557 Ryan. 1997. Property fields in an effluent plume of the Mississippi River, *J. Mar. Syst.*,
558 12, 109-126.

559 Jochens, A.E., S.F. DiMarco, W.D. Nowlin, Jr., R.O. Reid, M.C. Kennicutt, II. 2002.
560 Northeastern Gulf of Mexico Chemical Oceanography and Hydrography Study:
561 Synthesis Report. U.S. Department of the Interior, Minerals Management Service, Gulf
562 of Mexico OCS Region, New Orleans, LA, OCS study MMS 2002-055.

563 Justić D., N.N. Rabalais and R.E. Turner. 2003. Simulated responses of the Gulf of Mexico
564 hypoxia to variations in climate and anthropogenic nutrient loading. *J. Mar. Syst.* 42,
565 115–26.

566 Justić D, V.J. Bierman, D. Scavia and R.D. Hetland. 2007. Forecasting gulf's hypoxia: the next
567 50years? *Estuaries.* 30(5), 791–801.

568 Kemp, W. M., J. M. Testa, D. J. Conley, D. Gilbert and J. D. Hagy. 2009. Temporal responses of
569 coastal hypoxia to nutrient loading and physical controls. *Biogeosciences*, 6, 2985-3008

570 Kourafalou, V.H. and Y.S. Androulidakis. 2013. Influence of Mississippi River induced
571 circulation on the Deepwater Horizon oil spill transport. *J. Geophys. Res.:*
572 *Oceans*, 118(8), 3823-3842.

573 Lehrter J.C., M.C. Murrell and J.C. Kurtz. 2009. Interactions between freshwater input, light, and
574 phytoplankton dynamics on the Louisiana continental shelf. *Cont. Shelf Res.* 29(15),
575 1861-1872.

576 Liu, Y., M.A. Evans and D. Scavia. 2010. Gulf of Mexico hypoxia: Exploring increasing
577 sensitivity to nitrogen loads. *Environ. Sci. Tech.* 44(15), 5836–5841.

578 Morey, S.L., Schroeder, W.W., O'Brien, J.J. and Zavala-Hidalgo, J., 2003a. The annual cycle of
579 riverine influence in the eastern Gulf of Mexico basin. *Geophys. Res. Lett.*, 30(16), 1867,
580 doi:10.1029/2003GL017348.

581 Morey, S.L., P.J. Martin, J.J. O'Brien, A.A. Wallcraft and J. Zavala-Hidalgo. 2003b. Export
582 pathways for river discharged fresh water in the northern Gulf of Mexico. *J. Geophys.*
583 *Res.*, 108(C10), 3303, doi:10.1029/2002JC001674.

584 Milroy, S, 2016. Frequency of hypoxia at artificial reefs within the Mississippi Sound and Bight,
585 Jun-Oct 2016. In Abstracts of the 2016 Bays and Bayous Symposium, Biloxi, MS, Nov
586 30-Dec 1, 2016.

587 Moshogianis, A., J. Lopez, T. Henkel, E. Boyd, A. Baker and E. Hillmann. 2013. Preliminary
588 results of recently observed hypoxia development in the Chandeleur Sound and Breton
589 Sound of southeastern Louisiana, East of the Mississippi River Delta. Technical Report,
590 Lake Pontchartrain Basin Foundation, New Orleans, LA.

591 Nittrouer, J.A., J. Shaw, M.P. Lamb and D. Mohrig, 2012. Spatial and temporal trends for water-
592 flow velocity and bed-material sediment transport in the lower Mississippi River. *Bulletin*
593 *of the Geological Society of America*, 124(3-4), 400-414

594 Oviatt, C., L. Smith, J. Krumholz, C. Coupland, H. Stoffel, A. Keller, M. C. McManus, and L.
595 Reed. 2017. Managed nutrient reduction impacts on nutrient concentrations, water clarity,
596 primary production, and hypoxia in a north temperate estuary. *Estuarine, Coastal and*
597 *Shelf Science*, 199, 25-34.

598 Rabalais, N. N., R. E. Turner, D. Justić, Q. Dortch, and W.J. Wiseman. 1999. Characterization
599 of Hypoxia: Topic 1 Report for the Integrated Assessment on Hypoxia in the Gulf of
600 Mexico. NOAA Coastal Ocean Program Decision Analysis Series No 15. Silver Spring,
601 MD: NOAA Coastal Ocean Program; 167 pp.

602 Rabalais, N.N., R.E. Turner and W.J. Wiseman Jr. 2002a. Gulf of Mexico hypoxia, aka “The
603 dead zone”. *Annu. Rev. Ecol. and Syst.*, 33(1), 235-263.

604 Rabalais, N.N., R.E. Turner and D. Scavia. 2002b. Beyond science into policy: Gulf of Mexico
605 hypoxia and the Mississippi River: Nutrient policy development for the Mississippi River
606 watershed reflects the accumulated scientific evidence that the increase in nitrogen
607 loading is the primary factor in the worsening of hypoxia in the northern Gulf of Mexico.
608 *BioSci.*, 52(2), 129-142.

609 Rabalais N.N., R.E. Turner, B.K. Sen Gupta, D.F. Boesch, P. Chapman and M.C. Murrell. 2007
610 Hypoxia in the northern Gulf of Mexico: Does the science support the plan to reduce,
611 mitigate, and control hypoxia? *Estuaries Coasts*. 30(5), 753–772.

612 Rabalais, N.N., R.E. Turner, R.J. Diaz and D. Justić. 2009. Global change and eutrophication of
613 coastal waters. *ICES J. Mar. Sci.*, 66(7), 1528-1537.

614 Rakocinski, C.F. and D.P. Menke. 2016. Seasonal hypoxia regulates macrobenthic function and
615 structure in the Mississippi Bight. *Mar. Pollut. Bull.*, 105(1), 299-309.

616 Riemann, B., J. Carstensen, K. Dahl, H. Fossing, J.W. Hansen, H.H. Jakobsen, A.B. Josefson, D.
617 Krause-Jensen, S. Markager, P.A. Staehr, K. Timmermann, J. Windolf, J.H. Andersen.
618 2016, Recovery of Danish coastal ecosystems after reductions in nutrient loading: A
619 holistic ecosystem approach. *Estuaries Coasts*, 39, 82-97.

620 Rowe, G.T. and P. Chapman. 2002. Continental shelf hypoxia: some nagging questions. Gulf of
621 Mexico Science. 20(2), 8 153-160.

622 Sanial, V., A. Shiller, D. Joung, and P. Ho, submitted. Extent of Mississippi River water in the
623 Mississippi Bight and Louisiana Shelf based on water isotopes. *Estuarine, Coastal and*
624 *Shelf Science*, submitted.

625 Scavia, D., N.N. Rabalais, R.E. Turner, D. Justić and W.J. Wiseman Jr. 2003. Predicting the
626 response of Gulf of Mexico hypoxia to variations in Mississippi River nitrogen load.
627 *Limnol. Oceanogr.* 48(3),951–956.

628 Scavia,D., D. Justić and V.J. Bierman Jr. 2004. Reducing hypoxia in the Gulf of Mexico: Advice
629 from three models. *Estuaries* 27(3), 419–425.

630 Scavia, D., I. Bertani, D.R. Obenour, R.E. Turner, D.R. Forrest and A. Katin. 2017. Ensemble
631 modeling informs hypoxia management in the northern Gulf of Mexico. *Proc. Natl. Acad.*
632 *of Sci. U. S. A.*, 114(33), 8823-8828.

633 Schiller, R.V., V.H. Kourafalou, P. Hogan and N.D. Walker. 2011. The dynamics of the
634 Mississippi River plume: Impact of topography, wind and offshore forcing on the fate of
635 plume waters. *J. Geophys. Res.: Oceans*, 116, C06029, doi:10.1029/2010JC006883.

636 Staehr, P. A., J. Testa and J. Carstensen. 2017. Decadal Changes in Water Quality and Net
637 Productivity of a Shallow Danish Estuary Following Significant Nutrient Reductions.
638 *Estuaries Coasts*, 40, 63-79.

639 Turner, R.E., W.W. Schroeder and W.J. Wiseman 1987. The role of stratification in the
640 deoxygenation of Mobile Bay and adjacent shelf bottom waters. *Estuaries Coasts*, 10(1),
641 13-19.

642 Turner R. E. and N.N. Rabalais. 1994 Coastal eutrophication near the Mississippi river delta.
643 Nature. 368, 619–621.

644 Turner, R. E., N.N. Rabalais, R.B. Alexander, G. McIsaac and R.W. Howarth. 2007.
645 Characterization of nutrient and organic carbon, and sediment loads and concentrations
646 from the Mississippi River into the northern Gulf of Mexico. *Estuaries Coasts* 30,773–
647 790.

648 Turner, R.E., N.N. Rabalais and D. Justić. 2012. Predicting summer hypoxia in the northern Gulf
649 of Mexico: redux. *Mar. Pollut. Bull.* 64, 319–324.

650 U.S. Army Corps of Engineers, 1974. Deep Draft Access to the Ports of New Orleans and Baton
651 Rouge. Draft Environmental Statement, Corps of Engineers, New Orleans District.

652 Walker, N.D., L.J. Rouse Jr., G.S. Fargion and D.C. Biggs. 1994. The great flood of summer
653 1993: Mississippi River discharge studied. *Eos Transactions, AGU*, 75(36), 409-415.

654 Walker, N.D. 1996. Satellite assessment of Mississippi River plume variability: Causes and
655 predictability. *Rem. Sensing Env.*, 58(1), 21-35.

656 Walker, N.D., W.J. Wiseman Jr., L.J. Rouse Jr. and A. Babin. 2005. Effects of river discharge,
657 wind stress and slope eddies on circulation and the satellite-observed structure of the
658 Mississippi River plume. *J. Coastal Res.* 21, 1228-1244.

659 Walker, N.D. and N.N. Rabalais. 2006. Relationships among satellite chlorophyll *a*, river inputs
660 and hypoxia on the Louisiana continental shelf, Gulf of Mexico. *Estuaries Coasts*, 29
661 (6B), 1081-1093.

662 Weisberg, R.H. (1994). Transport of Mississippi River water to the west Florida shelf. In *Coastal*
663 *Oceanographic Effects of Summer 1993 Mississippi River Flooding*, edited by M.J.
664 Dowgiallo, Special Report, NOAA Coastal Ocean Office, pp. 55-59.

665 Wiseman, W.J., N.N. Rabalais, R.E. Turner, S.P. Dinnel and A.N. MacNaughton. 1997. Seasonal
666 and interannual variability within the Louisiana coastal current: stratification and
667 hypoxia. *J. of Mar. Syst.*, 12(1-4), 237-248.
668